Arthritis and Rheumatology in press

Chondrocytes play a role in the development of rheumatoid arthritis via TMEM147-mediated NF-κB activation

Mitsutoshi Ota[1, 2], Yuki Tanaka[1], Ikuma Nakagawa[1], Jing-Jing Jiang[1], Yasunobu Arima[1], Daisuke Kamimura[1], Tomohiro Onodera[2], Norimasa Iwasaki[2], Masaaki Murakami[1].

[1] Division of Molecular Psychoimmunology, Institute for Genetic Medicine, Graduate School of Medicine, Hokkaido University, Sapporo, Japan
[2] Department of Orthopaedic Surgery, Hokkaido University Graduate School of Medicine, Sapporo, Japan

Address corresponded to:
Masaaki Murakami
N15, W7, Kita-Ku, Sapporo, Hokkaido 060-0815, Japan
Phone : +81-11-706-5120
Fax : +81-11-706-7542
e-mail : murakami@igm.hokudai.ac.jp

ABSTRACT

Objective We previously reported that the co-activation of NF-κB and STAT3 in non-immune cells including synovial fibroblasts enhances the expression of NF-κB target genes, playing a role in chronic inflammation including rheumatoid arthritis (RA). Here we examined the role of NF-κB activation in chondrocytes to understand the pathogenesis of RA. Furthermore, we investigated TMEM147 as a representative NF-κB activator in chondrocytes.

Methods Clinical samples from RA patients were analyzed by immunohistochemistry. Samples from polydactyly patients served as a control. The functional contribution of chondrocytes and TMEM147 to arthritis was examined in several mouse RA models. In vitro experiments including qPCR, RNA interference, immunoprecipitation and confocal microscopy were performed to investigate the mechanism of action of TMEM147 in chondrocytes.

Results Samples from RA patients and from the RA models showed co-activation of NF-κB and STAT3 in chondrocytes. This co-activation induced a synergistic expression of NF-κB targets in vitro. Chondrocyte-specific deletion of STAT3 significantly suppressed the development of cytokine-induced arthritis. TMEM147 was highly expressed in chondrocytes from RA patients and the RA models. Gene silencing of TMEM147 or anti-TMEM147 antibody treatment inhibited the cytokine-mediated activation of NF-κB in vitro and suppressed the cytokine-induced arthritis in vivo. Mechanistically, TMEM147 molecules acted as a scaffold protein for a NF-κB complex that included breakpoint cluster region and casein kinase 2 to enhance NF-κB activity.

Conclusion These results suggest that chondrocytes play a role in the development of RA via TMEM147-mediated NF-κB activation and provide a novel therapeutic strategy for RA.

KEYWORDS

Rheumatoid arthritis, Chondrocytes, Inflammation, Cytokines, NF-κB, TMEM147

INTRODUCTION

Cartilage is an essential component of the synovial joints and is composed of chondrocytes. Cartilage shows extremely high durability in healthy conditions, but also has poor natural healing ability. Therefore, once it is damaged, it gradually deteriorates to ultimately dysfunction [1]. Rheumatoid arthritis (RA) is a chronic inflammatory disease that causes joint destruction [2]. In RA, cartilage is considered a target tissue for synovial inflammation [3]. Indeed, during RA development, cytokines expressed from immune cells and fibroblast-like synoviocytes damage the cartilage tissue by promoting the production of matrix metalloproteinases (MMPs) and aggrecanases (ADAMTS families) from the chondrocytes [4 5]. Chondrocytes secrete MMPs and ADAMTS families after stimulation with CXCL6 and FGF-2, leading to their dysfunction {Kawaguchi, 2008 #38;Pap, 2015 #9;Sanchez, 2017 #10}. On the other hand, it is reported that heterozygous knockout of NF-κB p65 or ADAMTS5 deficiency in chondrocytes retards the development of an osteoarthritis model via catabolic inhibition or of an antigen-induced arthritis model, respectively {Kobayashi, 2016 #47;Stanton, 2005 #48}. At the same time, the homozygous knockout of NF-κB p65 in chondrocytes enhances the development of osteoarthritis via chondrocyte apoptosis [6]. As a result, the role of the NF-κB pathway in chondrocytes remains controversial during RA development.

Although inflammation is an important biological defense, chronic inflammation is known to cause metabolic diseases, neurodegenerative diseases and autoimmune diseases including RA [6-8]. As a key molecular mechanism in chronic inflammation, we previously reported the inflammation amplifier, which was originally termed the IL-6 amplifier [9 10]. The inflammation amplifier is a hyper NF-κB activation machinery in non-immune cells including synovial fibroblasts induced by the simultaneous activation of NF-κB and STAT3. It induces a massive and sustained production of NF-κB target genes, including IL-6, chemokines, and growth factors, which is critical for the development of various disease models including RA [9 10]. Furthermore, we have shown that the co-activation of NF-κB and STAT3, which is evidence of activation of the inflammation amplifier, is observed in clinical specimens from patients with inflammatory diseases [11 12]. Additionally, the expression of target molecules of the inflammation amplifier is higher in the serum of patients with RA or multiple sclerosis {Murakami, 2013 #6;Harada, 2015 #3}. These findings suggest a new therapeutic strategy based on the amplifier. Accordingly, we conducted a shRNA-based genome wide screening, in which we identified more than 1,000 genes involved in activation of the inflammation amplifier [8]. In particular, we reported that BCR, which is known to form the oncogenic fusion protein BCR-Abl [13], interacts with the α subunit of casein kinase II (CK2α), leading to the phosphorylations of BCR at tyrosine 177 and NF-κB p65 at serine 529 to transcriptionally activate NF-κB p65 in the nucleus following TNF-α stimulation. Thus, the formation of the BCR-CK2α-NF-κB p65 complex in the cytoplasmic region plays a role in nuclear function of NF-κB [14].

In the present study, we focused on transmembrane protein 147 (TMEM147) as a positive regulator of NF-κB, because of its high expression in chondrocytes in the inflamed area. TMEM147 is a seven-transmembrane protein whose functions are not well known [15]. We here demonstrated the importance of chondrocytes in amplifying inflammatory responses during RA development based on the following six observations: (i) chondrocytes and a chondroprogenitor cell line, ATDC5, synergistically expressed NF-κB targets after stimulation with TNF-α or IL-17 plus IL-6, (ii) chondrocytes in RA patients and in mouse models of RA showed the simultaneous activation of NF-κB and STAT3, (iii) chondrocytes deficient of STAT3 suppressed the development of the RA model, (iv) the deficiency or blockade of TMEM147 molecules suppressed the expression of NF-κB targets in vitro and in vivo, (v) TMEM147 acted as a scaffold protein for the BCR/CK2α-mediated NF-κB activation pathway, and (vi) anti-TMEM147 antibody injections in the joints suppressed the development of the RA model. These findings reveal a novel role for chondrocytes in RA

96 development via TMEM147-dependent NF-κB activation.
97

MATERIALS AND METHODS

Mouse Strains

C57BL/6 mice were purchased from Japan SLC (Shizuoka, Japan). The F759 (gp130$^{F759/F759}$ knock-in) mouse line was previously established [16]. Col2a1-Cre mice (B6; SJL-Tg [Col2a1-Cre] 1Bhr/J) were obtained from the Jackson Laboratory (Bar Harbor, ME) and crossed with STAT3flox/flox mice that were provided by S. Akira (Osaka University, Japan) [17]. All animal experiments performed in this study were approved by Hokkaido University, Institute for Genetic Medicine, Japan, and all mice were housed and maintained under specific pathogen-free conditions according to the institute's animal care guidelines. Animal experiments were performed following the guidelines of the Institutional Animal Care and Use Committees of Hokkaido University. The protocols for animal experiments were approved by the Institutional Animal Care and Use Committees of Hokkaido University.

Spontaneous RA models

F759 mice [16 18] (12-months old) were euthanized, and their entire ankle joints were dissected for examinations.

Cytokine-induced arthritis models

Human IL-6 (100 ng, Toray Industries, Tokyo, Japan), mouse IL-17A (100 ng, R&D Systems, Tokyo, Japan) or saline was injected into the ankle joints of F759 mice, as described previously [19]. In some experiments, lentivirus particles carrying short hairpin RNA (shRNA) specific for TMEM147 (Sigma-Aldrich, Tokyo, Japan) or a scrambled sequence (Sigma-Aldrich) were injected into the ankle joints of the mice [8 14 19-23]. Anti-TMEM147 antibodies (Sigma-Aldrich) were injected into the ankle joints of mice at a dose of 2 μg/day. The same dosage of rabbit IgG (Santa Cruz Biotechnology, Tokyo, Japan) served as a control. Clinical signs of arthritis were evaluated, as described previously [19]. In brief, the severity of the arthritis was determined based on restricted mobility of the ankle joints with a scale of 0–3, where 0 indicates no change; 1, mild change; 2, medium change; and 3, severe change. Averages for a single point in one leg ankle joint from each mouse were used. The mice were euthanized, and their entire ankle joints were dissected for the examinations.

Spontaneous OA models

C57BL/6 mice [24] (24 months old) were euthanized, and their entire ankle joints were dissected for the examinations.

Collagen-induced arthritis models

C57BL/6 mice (8 months old) were immunized with CFA plus type I collagen peptide (sequences?), and their entire ankle joints were dissected for the examinations.

Clinical specimens

RA patients (n = 6) and OA patients (n = 5) undergoing total knee arthroplasty (TKA) surgery, and polydactyly patients (control; n = 5) undergoing reconstruction surgery at Hokkaido University Hospital, Sapporo, Japan, were recruited to the study after written informed consent (Supplementary Table 1). Every patient with RA fulfilled the American College of Rheumatology criteria for the classification of RA {Aletaha, 2010 #42}, and every patient with OA was classified with Kellgren-Lawrence grade 3 or 4 {Kellgren, 1957 #46}. Sample collection, processing, storage and subsequent experimental procedures were carried out in compliance with Human Tissue Authority guidelines under the Human Tissue Act (2004). The study protocol was approved by the Human Ethics Committee of Hokkaido University Hospital and was conducted in accordance with the Declaration of Helsinki Principles. All patient identifiers were removed from the data.

147
148 **Cells and stimulation conditions**
149 A chondroprogenitor cell line, ATDC5, was obtained from Riken Cell Bank (Ibaraki, Japan). Primary
150 murine chondrocytes were prepared from newborn mice, as described previously [25]. Primary human
151 chondrocytes were sourced from non-pathologic articular cartilage (Cell Applications Inc., San
152 Diego, CA, USA). Cells were plated in 96-well flat-bottom plates or 100 mm dishes and stimulated
153 with human IL-6 plus soluble human IL-6Rα (100 ng/mL each; Toray Industries) and/or mouse or
154 human IL-17A (50 ng/mL; R&D Systems) as well as mouse or human TNF-α (50 ng/ml; PeproTech,
155 Tokyo, Japan) after 2 hr serum starvation. Anti-TMEM147 antibody (20 ng/mL; Sigma-Aldrich) was
156 added to some experiments. Mouse cells are responsive to human IL-6 which allowed us to measure
157 mouse IL-6 in the culture supernatant after stimulation with human IL-6 and mouse IL-17A using
158 mouse-specific IL-6 ELISA (eBioscience and BD Biosciences, Tokyo, Japan).
159
160 **TMEM147 shRNA knockdown cells**
161 ATDC5 cells were cultured on day 0 in a 96-well flat-bottom plate (1 x 10^3 cells/well) in 100 µL of
162 DMEM/F-12 (1:1) with 2 mM L-Glutamine containing 5% FBS. The medium was replaced on day 1
163 with DMEM/F-12 (1:1) containing lentivirus carrying 1 µL of candidate-specific shRNA
164 (TMEM147 shRNA, TRCN0000174842; non-target shRNA, SHC002; Sigma-Aldrich), 5% FBS and
165 8 µL/mL Polybrene. 200 µL of DMEM/F-12 (1:1) containing 5% FBS and 5 µg/mL puromycin was
166 added to each well on day 2. Cells that survived drug selection with puromycin were designated as
167 TMEM147 knockdown cells and the knockdown efficiency was verified by qPCR and Western
168 blotting.
169
170 **Human small interfering RNAs**
171 Primary human chondrocytes were cultured on day 0 in a 96-well flat-bottom plate (7 x 10^3
172 cells/well) in 100 µl of Human Chondrocyte Media (Cell Applications Inc.). A mixed solution of
173 Opti-MEM (18 µL/well, Thermo Fisher Scientific, Kanagawa, Japan), 5 µM small interfering RNAs
174 (siRNAs) and Lipofectamine RNAiMAX (0.28 µL/well, Thermo Fisher Scientific) was added into
175 the culture medium on day 1. The medium was replaced on day 2 with Human Chondrocyte Media
176 (Cell Applications Inc.). The knockdown efficiency was verified by qPCR, and the sequences for the
177 sense oligonucleotides of the most effective knockdown constructs were as follows: human
178 siTMEM147 (s20403; Thermo Fisher Scientific) and human non-target (SIC-001; Sigma-Aldrich).
179
180 **Plasmids**
181 The Flag-tagged murine TMEM147 expression vector was constructed as follows.
182 TMEM147-encoding cDNA was synthesized from the total cellular RNA of ATDC5 cells using KOD
183 FX (TOYOBO, Osaka, Japan) for RT-PCR with a primer pair. The cDNA was electrophoresed on
184 2.5% agarose gel and extracted. The cDNA and pCMV-Tag2B were treated with restriction enzymes
185 (BamH I, Sal I, High buffer, TaKaRa) at 37 ˚C for 2.5 hr and ligated with ligation buffer (Ligation
186 high Ver 2, TOYOBO) at 16 ˚C for 2 hr. The prepared vector was transfected into competent cells
187 (ECOS DH5α, NIPPON GENE) and cultured in 100 mm LB Agar plate containing kanamycin (20
188 µg/mL) overnight at 37 ˚C. The colonies generated by drug selection with kanamycin were picked up
189 and cultured in 100 mL LB medium containing kanamycin (20 µg/mL) overnight at 37 ˚C in an
190 incubator shaker (EYLA, Tokyo, Japan). The GenElute HP Plasmid Midiprep Kit (Sigma-Aldrich)
191 was used to extract plasmid DNA from the culture medium. The presence of the intended fragment
192 without any unexpected mutations was confirmed by DNA sequencing with a BigDye Terminator
193 v3.1 Kit (Applied Biosystems, Tokyo, Japan). All primers are listed in Supplementary Table 2.
194
195 **Antibodies**

The following antibodies (Abs) were used for western blotting, immunoprecipitation, qPCR, ELISA, confocal microscopy, immunohistochemistry, flow cytometry, or joint injection: anti-TMEM147 (sc-138814, Santa Cruz Biotechnology), anti-TMEM147 (generated by immunizing rabbit with peptide containing amino acids 121-136 VGARGIEFDWKYIQMSC, Sigma-Aldrich), anti-NF-κB p65 (sc-372, Santa Cruz Biotechnology), anti-phospho-p65 S536 (#3033, Cell Signaling Technology, Tokyo, Japan), anti-phospho NF-κB p65 S529 (ab47395, Abcam, Tokyo, Japan), anti-phospho NF-κB p65 S276 (SAB4504488, Sigma-Aldrich), anti-phospho-stat3 (#9145, Cell Signaling Technology), anti-IκBα (#4814, Cell Signaling Technology), anti-phospho-IκBα (#9246, Cell Signaling Technology), anti-BCR (#3902, Cell Signaling Technology), anti-phospho-BCR Y177 (#3901, Cell Signaling Technology), anti-CK2α (#2656, Cell Signaling Technology), anti-phospho-CK2α (SAB4300628, Sigma-Aldrich), anti-α-tubulin (T5168, Sigma-Aldrich), anti-FLAG M2 (F1804, Sigma-Aldrich), rabbit IgG (#3900, Cell Signaling Technology), anti-rabbit IgG (sc-2004, Santa Cruz Biotechnology), anti-mouse IgG (sc-2314, Santa Cruz Biotechnology), anti-goat IgG (sc-3851, Santa Cruz Biotechnology), Alexa Fluor 488 goat anti-rabbit IgG (H+L) (A11055, Life technologies, Tokyo, Japan) and Hoechst 33342 trihydrochloride trihydrate (H3570, Life technologies).

Quantitative real-time PCR (qPCR)

Total RNA was isolated from the cells using the SuperPrep Cell Lysis Kit for qPCR (Toyobo, Osaka, Japan) and was isolated from the tissue using ISOSPIN Cell & Tissue RNA (NIPPON GENE, Toyama, Japan). cDNAs were made using M-MLV Reverse Transcriptase (Promega, Tokyo, Japan). mRNA levels were quantified by qPCR using ABI Prism 7300 fast real-time PCR system (Applied Biosystems, Tokyo, Japan) and SYBR Green FAST qPCR master mix (Kapa Biosystems, Woburn, MA). The conditions for real-time PCRs were 40 cycles at 94 ˚C for 15 sec followed by 40 cycles at 60 ˚C for 60 sec. The relative mRNA expression levels were normalized to the levels of HPRT or GAPDH mRNA expression. All primers are listed in Supplementary Table 2.

Enzyme-linked immunosorbent assay (ELISA) and MTT assay

Cells were plated in 96-well flat-bottom plates and cultured overnight on day 0. On day 1, cell stimulation was conducted for 24 hr under the conditions described above. The culture supernatant was collected and mouse IL-6 concentrations were determined using ELISA kits specific for mouse IL-6 (BD Biosciences). 100 μL of 3-(4,5-dimethylthiazol-2-yl)-2,5-diphenyltetrazolium bromide (MTT)-containing DMEM (500 μg/mL) was added to the cells after ELISA, and the color reaction was carried out by culturing at 37 ˚C for 2 hr. After removal of the culture supernatant, the produced formazan was dissolved in 100 μL DMSO. The absorbance was measured with a Model 680 Microplate Reader (BIO RAD, Tokyo, Japan).

Western blotting

Mock (non-target control), TMEM147 knockdown cells and cells which were forced to express TMEM147 were lysed with HBST (0.5) lysis buffer (0.5% TritonX-100, 150 mM NaCl, 10 mM HEPES [pH7.4]) containing 1/100 volume of protease inhibitor mixture, phosphatase inhibitor mixture 2 and phosphatase inhibitor mixture 3 (Sigma-Aldrich). The protein lysates were heated only to 60 °C to avoid the aggregation of TMEM147. 20 μg of total protein was run on 5-20% SDS-PAGE (Wako, Tokyo, Japan). After transfer to a polyvinylidene fluoride membrane (Pall Corporation, Port Washington, NY), immunoblotting was performed according to the manufacturer's protocol.

Immunoprecipitation

The protein lysates, which were adjusted to 1 mg/mL for immunoprecipitation, were assessed

pre-clear with 30 µL of protein G Sepharose to remove non-specific binding proteins (17-0618-02, GE Healthcare, Tokyo, Japan) and incubated for 1 hr at 4 °C with gentle agitation. The supernatant was mixed with 30 µL of anti-Flag beads (A2220, Sigma-Aldrich, Tokyo, Japan), followed by rotation for 2 hr at 4 °C. For the detection of p65 S529 phosphorylation, the supernatant was mixed with 2 µg of anti-p65 Ab, which was immobilized on protein G Sepharose, followed by rotation for 2 hr at 4°C. The immunoprecipitates were eluted with 3X Flag peptide (F4799, Sigma-Aldrich) or 2X SDS-PAGE loading buffer, separated by SDS-PAGE, and transferred to a polyvinylidene difluoride membrane followed by Western blotting with the antibodies, as previously described (references).

Luciferase Assay

pGL4.32[luc2P/NF-κB-RE/Hygro] or IL-6-RE cloned into pGL4.20[luc2P/Puro] vector and pRL-TK vector (Promega, Tokyo, Japan), and pCMV-Tag2B vector containing cDNA for TMEM147 were transiently co-transfected into HEK293T cells by using polyethylenimine (PEI). Cells cultured in 96-well flat-bottom plates were harvested after 24 hr transfection and stimulated with TNF-α (50 ng/mL; PeproTech, Tokyo, Japan) for 6 hr. Luciferase activities of total cell lysates were measured using a Dual-Luciferase reporter assay system (Promega, Tokyo, Japan) and Glomax-Multi Detection System (Promega, Tokyo, Japan).

Confocal laser scanning microscopy

Mock (non-target control) and TMEM147 knockdown cells were stimulated with TNF-α for 0, 15, and 30 min on µ-Slides (Ibidi, Martinsried, Germany). The stimulated cells were fixed and permeabilized with a Cytofix/Cytoperm Kit (BD Biosciences), and incubated with rabbit anti-p65 (1 µg/mL) for 1 hr at 4 °C. After washing, the cells were incubated with anti-rabbit Alexa Fluor 488-conjugated secondary Ab (10 µg/mL) and Hoechst 33342 nuclear stain (1 µg/mL) for 1 hr at 4 °C. Cells were then observed by confocal microscopy (LSM5 Pascal system, Zeiss, Tokyo, Japan).

Cell surface flow cytometry analysis

The cell surface expression of TMEM147 on ATDC5 cells was detected using generated anti-TMEM147 Ab (1 µg/mL). The secondary detection antibody used was anti-rabbit Alexa Fluor 488-conjugated Ab (10 µg/mL). Control IgG was used at the same concentrations. Non-specific binding was blocked with the Fc block (10-20 µg/mL; BD Biosciences) before antibody staining. For all flow cytometry experiments, cells were stained for 30 min at 4 °C in the dark and washed three times with flow cytometry buffer (PBS + 1% FBS). Samples were analyzed using CyAn^{TM} ADP (BECKMAN COULTER, Tokyo, Japan). Data were analyzed with FlowJo software (BD Biosciences).

Statistical analysis

Student's t tests (two-tailed) were used for the statistical analyses of differences between two groups. One-way ANOVA with Dunnett's post hoc analysis was used for multiple comparisons. Wilcoxon rank-sum test was used for the statistical analyses of clinical scores of the arthritis model. *P* values less than 0.05 were considered significant (*$P < 0.05$, **$P < 0.01$, and ***$P < 0.001$).

RESULTS

Enhanced NF-κB activation in chondrocytes plays an important role in the pathogenesis of RA mouse models

We first investigated whether the inflammation amplifier is activated in the chondrocytes of synovial joints. Activation was monitored by the enhanced expression of NF-κB targets such as IL-6 [8 9 11 12 14 19-23 27 28]. Murine primary chondrocytes were prepared [25] and stimulated with IL-6, IL-17A and/or TNF-α. IL-6 mRNA and protein levels were significantly increased in chondrocytes (Fig. 1A and 1B). The expression of MMP13 and ADAMTS5 also increased after cytokine stimulation in chondrocytes (Fig. S1). The mouse chondroprogenitor cell line ATDC5 also showed the synergistic production of IL-6 after cytokine treatment (Fig. S2).

We then investigated whether the activation of NF-κB and STAT3 can be observed in inflamed joints. We first employed F759 knock-in mice (12-months old) as a RA model, because they spontaneously develop RA-like arthritis with age due to exaggerated IL-6 signaling caused by the lack of a SOCS3-binding site on the IL-6 receptor gp130 [16 18]. In older F759 mice, cartilage tissue denaturation was observed with Safranin-O staining, and the activation of NF-κB and STAT3 was confirmed in the chondrocytes (Fig. 1C-1E). Consistent with this observation, bone destruction was clearly observed by using computed tomography (CT) analysis (Fig. S3A and S3H), and the knee joints were similarly affected (Fig. S4A-S4C). F759 mice with chondrocyte-specific deletion of STAT3 were generated using Col2a1 promoter-driven cre mice, which prevents the co-activation of NF-κB and STAT3 in chondrocytes. Because RA-like arthritis in F759 mice is dependent on the age-dependent increase of IL-6 and IL-17 from Th17 cells [27], direct articular injections of IL-6 and IL-17 accelerated the arthritis induction to within two weeks [8 9 14 19-23]. This cytokine-induced arthritis was significantly suppressed in Col2a1-STAT3$^{fl/fl}$ F759 mice (Fig. 1F). Synovial hyperplasia, cartilage degeneration, and the activation of NF-κB and STAT3 were suppressed in Col2a1-STAT3$^{fl/fl}$ F759 mice according to histological analysis (Fig. S5A-S5C). In the cytokine-induced arthritis model, bone erosion was not detected in 8-week-old mice, most likely because of their young age (Fig. S3). Soft tissue swelling was suppressed, and bone destruction was reduced in 12-month-old Col2a1-STAT3$^{fl/fl}$ F759 mice (Fig. S3D, S3E, S3H and S3I). Thus, enhanced NF-κB activation in chondrocytes has a crucial pathogenic role in the development of arthritis in RA models.

Enhanced activation of NF-κB in chondrocytes was observed in RA patients

We next investigated whether activation of the inflammation amplifier also occurs in RA patients. The expression of IL-6 mRNA was significantly increased in human primary chondrocytes stimulated with IL-6 plus IL-17A or TNF-α (Fig. 2A). The joint cartilage of RA patients was remarkably denatured, as judged by Safranin-O staining, and the activation of NF-κB and STAT3 was significantly enhanced in the chondrocytes (Fig. 2B and 2C).

TMEM147 is critical for NF-κB activation in chondrocytes

TMEM147, a candidate gene marker of inflammation amplifier activation [8], was clearly increased in chondrocytes in the ankle joints of F759 mice as well as RA patients (Fig. 3A and 3B). Similar results were observed in the knee joints of a mouse RA model and Col2a1-STAT3$^{fl/fl}$ F759 mice (Fig. S4D and S5D). ATDC5 cells with TMEM147 knockdown showed less IL-6 expression after IL-6 plus IL-17 stimulation (Fig. 3C-3F), while the forced expression of TMEM147 increased the reporter activity of NF-κB and IL-6 promoters (Fig. 3G and 3H) and enhanced IL-6 expression (Fig. S6). TMEM147 knockdown suppressed the expression other NF-κB target genes including CCL20 and CXCL1, but not a STAT3 target, STAT3 itself [29] (Fig. 3I), suggesting that TMEM147 controls the NF-κB pathway. Importantly, TMEM147 played a role in NF-κB activation in human primary chondrocytes (Fig. 3J-3L). Moreover, the clinical scores of the cytokine-induced arthritis was significantly suppressed by TMEM147 knockdown in the ankle joints (Fig. 3M). Synovial

hyperplasia and cartilage degeneration were suppressed in TMEM147 knockdown mice (Fig. S7). Soft tissue swelling was suppressed in TMEM147 knockdown mice, and bone destruction was not observed (Fig. S3F, S3G). These results suggested that TMEM147 is a positive regulator of NF-κB activation in chondrocytes in vitro and in vivo.

TMEM147 acts as a scaffold protein for the BCR-CK2α complex

We next investigated which step(s) of the NF-κB signaling pathway is positively regulated by TMEM147 molecules. The phosphorylation of NF-κB p65 at S536 as well as the phosphorylation and degradation of IκBα were not affected in TMEM147 knockdown cells after TNF-α stimulation (Fig. 4A). Consistently, there was no significant change in the nuclear translocation of NF-κB p65 between mock and TMEM147 knockdown cells (Fig. 4B). On the other hand, phosphorylations in the BCR-CK2α-NF-κB p65 pathway, including BCR at Y177, CK2α at Y360, and NF-κB p65 at S529, were diminished in TMEM147 knockdown cells (Fig. 4C-4E). Furthermore, TMEM147 molecules were associated with endogenous BCR and NF-κB p65, but not CK2α (Fig. 4F), and the association of BCR with NF-κB p65 was compromised in TMEM147 knockdown cells (Fig. 4G). These results suggested that TMEM147 acts as a scaffold protein to bind BCR with NF-κB p65 and is required for the downstream phosphorylation events mediated by the BCR-CK2α-NF-κB p65 pathway [14].

Antibody against TMEM147 suppressed the development of RA models

We then established an antibody against an extracellular domain of TMEM147 molecules (Fig. S8A). Anti-TMEM147 antibody suppressed the activation induced by IL-6 and IL-17A stimulation in ATDC5 cells (Fig. 5A-5C). Notably, joint injections of anti-TMEM147 antibody suppressed cytokine-induced arthritis (Fig. 5D). Furthermore, anti-TMEM147 antibody injections suppressed synovial hyperplasia, cartilage degeneration, and the activation of NF-κB and STAT3 as well as IL-6 mRNA expression in the joints (Fig. 5E-5G, S8B and S8C). Similar results were also obtained in a CIA model (Fig. S9). We were able to observe soft tissue swelling but no bone destruction in both models over a short observation period (Fig. S3J and S3K). Overall, these data strongly suggested that blockade of TMEM147-mediated signaling by an antibody has therapeutic value for RA models..

DISCUSSION

During RA development, along with immune cells, including lymphocytes, monocytes, neutrophils, etc., non-immune cells, including chondrocytes and fibroblasts, in the affected joints are involved in the pathogenesis. Chondrocytes express MMPs and ADAMTS families in the joints of RA patients, followed by the degradation of the cartilage [4 5 30]. However, clinical trials on MMP inhibitors have failed [30 31]. In addition, many biological products including antibody drugs have been used for RA therapy, but a cure remains elusive [2]. These facts suggest more study on the pathological mechanism is needed.

We found an enhanced production of cartilage-degrading enzymes including MMP13 and ADAMTS5 in chondrocytes (Fig. S1). Importantly, the conditional deletion of STAT3 in chondrocytes that abrogates the co-activation of NF-κB and STAT3 significantly suppressed the clinical symptoms of RA models in vivo (Fig. 1E, S3D, S3E, S3H, S3I and S4). These results indicated that chondrocytes contribute to the inflammation development in RA, most likely by expressing soluble factors, which may affect both immune cells and non-immune cells. We also demonstrated that TMEM147 molecules in chondrocytes are critical for the RA development through NF-κB activation, suggesting a new candidate therapeutic target for RA. Notably, we found the activation of NF-κB and STAT3 and the enhanced expression of TMEM147 molecules in osteoarthritis (OA) model mice and OA patients (Fig. S10-S12). Therefore, it is reasonable that the same TMEM147 pathway might play a role in the inflammation development both in RA and OA. In addition, other inflammatory joint diseases, such as psoriatic arthritis or gouty arthritis, may develop through similar mechanisms.

We have reported that many regulatory and target molecules of the inflammation amplifier could be new markers and therapeutic targets of RA [8 20]. In this study, we defined TMEM147 as a novel key molecule for the inflammation amplifier in chondrocytes. It is reported that TMEM147 functions as a binding partner with membrane proteins. Rosemond et al. reported that TMEM147 binds to M3 muscarinic acetylcholine receptor and acts as a negative regulator of the receptor function on ## cells [32]. Another study suggested that TMEM147 molecules are associated with the Nicalin-NOMO complex on ## cells [15]. In addition, TMEM147 localizes on the cell surface and is a binding partner of Haemonchus controtus galectin on goat peripheral blood mononuclear cells {Li, 2016 #45}, and the membrane-based split-ubiquitin yeast two-hybrid system identified CLN8 and glucagon-like peptide 1 receptor as binding partners of TMEM147 {Passantino, 2013 #25;Huang, 2013 #26}. However, it is not known whether TMEM147 is directly involved in the NF-κB pathway. There are many phosphorylation sites in NF-κB molecules (12). For example, the phosphorylation of p65 S276 is important for DNA binding (13), the phosphorylation of p65 S536 promotes binding with TFIID (14), and the phosphorylation of p65 S468 is important for p65 transactivation activity (15). We found that the BCR-CK2α complex together with TMEM147 phosphorylates p65 S529 to establish a binding site for the acetyltransferase p300 at the promoter region of NF-κB target genes, thus inducing NF-κB-specific transcription by acetylating NF-κB p65 at K310 and histone H3 at K27 (14)(Fig. 4F and 4G). Thus, we show a new role for TMEM147 as a scaffold protein in NF-κB signaling (Fig. 6).

We also found that an antibody directed at an extracellular domain of TMEM147 as well as TMEM147 deficiency by shRNA-lentivirus suppressed IL-6 production in vitro and RA-like arthritis development in vivo (Fig. 3, 5, S8 and S9). These results suggest that TMEM147-mediated NF-κB activation could be a therapeutic target of RA. We hypothesize that antibody binding to the extracellular region of TMEM147 may prevent efficient formation of the BCR-CK2α-NF-κB p65 complex intracellularly by sequestering TMEM147 from the cytokine receptor signaling components in chondrocytes, although we do not exclude the possibility that TMEM147 suppression in other cell

types including fibroblasts by the same antibody treatment might also contribute to the in vivo effects observed in this study. The precise mechanism of action requires further investigation.

In summary, our results highlighted the significant contribution of chondrocytes to the development of RA via TMEM147-mediated activation of the inflammation amplifier. This new function of TMEM147 may offer a novel therapeutic strategy for NF-κB-mediated inflammation in degenerative joint diseases such as RA.

Acknowledgments
We appreciate the excellent technical assistance provided by Ms. C. Nakayama and Ms. M. Ezawa, Mr. Takuto Ohki, and thank Ms. S. Fukumoto (Hokkaido University, Sapporo, Japan) for her excellence assistance. We thank Dr. P. Karagiannis (CiRA, Kyoto University, Kyoto, Japan) for carefully reading the manuscript. This work was supported by JSPS KAKENHI (D. K., Y. A., and M. M.), the Joint Usage/Research Center Institute for Genetic Medicine, Hokkaido University (M. M.), and Takeda Science Foundation (M. M.),

Author contribution
All authors were involved in drafting the article or revising it critically for important intellectual content, and all authors approved the final version to be published.
Study conception and design: Iwasaki and Murakami.
Manuscript writing: Ota, Kamimura, and Murakami.
Acquisition of data: Ota, Tanaka, Jiang, and Kamimura.
Analysis and interpretation of data: Ota, Tanaka, Nakagawa, Jiang, Arima, Kamimura, Onodera, Iwasaki and Murakami.

Figure legends

Figure 1. Enhanced activation of the inflammation amplifier in chondrocytes is important for RA development in mice.

(**A** and **B**) Murine primary chondrocytes were stimulated with human IL-6 plus sIL-6Rα and/or IL-17A or TNF-α, and mRNA (A) or protein (B) levels of IL-6 were measured. IL-6 production was measured by ELISA specific for mouse IL-6, which was not cross-reactive with human IL-6 added to the culture. Dot plots in (B) show cell growth measured by the MTT assay (right axis).

(**C**) Safranin-O staining and immunohistochemistry using anti-phospho-NF-κB p65 and phospho-STAT3 antibodies of the ankle in spontaneous RA model mice are shown (n = 5 per group). Scale bars: 100 μm.

(**D**) The percentage of Safranin-O (+) in the cartilage areas of (C).

(**E**) The percentages of cells showing phosphorylated NF-κB p65 and phosphorylated STAT3 in the cartilage areas. At least 200 cells were counted in each mouse.

(**F**) The cytokine-induced arthritis model was induced in F759 mice or Col2Cre+ STAT3 flox/flox mice by ankle joint injections of IL-6 and IL-17A on days 0-2. Clinical scores of the arthritis are shown (n = 4-8 per group).

Data represent the mean ± S.D. (A, B, D and E) or S.E.M. (F). * $p < 0.05$, ** $p < 0.01$ and *** $p < 0.001$. In vitro experiments were performed at least three times.

Figure 2. Enhanced activation of the inflammation amplifier is observed in chondrocytes from RA patients.

(**A**) Human primary chondrocytes were stimulated with IL-6 plus sIL-6Rα and/or IL-17A or TNF-α, and IL-6 mRNA expression was measured.

(**B**) Safranin-O staining and immunohistochemistry using anti-phospho-NF-κB p65 and phospho -STAT3 antibodies of knee joints in patients with polydactyly (control) or RA are shown (n = 5-6 per group). Scale bars: 100 μm.

(**C**) The percentage of cells showing phosphorylated NF-κB p65 and phosphorylated STAT3 in the cartilage areas. At least 200 cells were counted in each patient.

Data represent the mean ± S.D. * $p < 0.05$ and *** $p < 0.001$. In vitro experiments were performed at least three times.

Figure 3. TMEM147 controls the NF-κB signaling pathway.

(**A** and **B**) Safranin-O staining and immunohistochemistry using anti-TMEM147 antibody or control IgG of the ankle joints from spontaneous RA models (A) or from RA patients (B) are shown (n = 5-6 per group). Scale bars: 100 μm.

(**C** and **D**) TMEM147-deficient ATDC5 cells were established by using a lentivirus that encoded shRNA specific for TMEM147. The knockdown efficiency of mRNA (C) and protein (D) levels is shown.

(**E** and **F**) Control (Mock) and TMEM147-deficient ATDC5 (sh) cells were stimulated with or without human IL-6 plus sIL-6Rα and IL-17A, and mRNA (E) or protein (F) levels of IL-6 were measured. IL-6 production was measured by ELISA specific for mouse IL-6, which was not cross-reactive with human IL-6 added to the culture. Dot plots in (F) show cell growth measured by the MTT assay (right axis).

(**G** and **H**) Control (Mock) and TMEM147-overexpressing HEK293T cells were stimulated with or without TNF-α. Reporter activities of NF-κB (G) and IL-6 (H) promoters are shown.

(**I**) Control (Mock) and TMEM147-deficient ATDC5 (sh) cells were stimulated with human IL-6 plus sIL-6Rα and IL-17A, and mRNA levels of CCL20, CXCL1 and STAT3 were measured.

(**J**) TMEM147-deficient human primary chondrocytes were established by using TMEM147-specific siRNA. The knockdown efficiency of TMEM147 at the mRNA level in the presence or absence of

human IL-6 plus sIL-6Rα and TNF-α stimulation is shown.
(**K**) Control (si-Control) and TMEM147-deficient (si) human primary chondrocytes were stimulated with or without human IL-6 plus sIL-6Rα and TNF-α. IL-6 mRNA levels were measured.
(**L**) Control (si-Control) and TMEM147-deficient (si) human primary chondrocytes were stimulated with human IL-6 plus sIL-6Rα and TNF-α, and the mRNA levels of CCL2, CXCL1 and STAT3 were measured.
(**M**) The cytokine-induced arthritis model that received ankle injections of lentivirus carrying non-target control shRNA sequence (Mock), shRNA specific to TMEM147 (sh TMEM147) or NF-κB p65 (sh p65, a positive control) before IL-6 and IL-17A stimulation. Clinical scores of the arthritis are shown (n = 4-8 per group).
Data represent the mean ± S.D. (C, E-L) or S.E.M. (M). * $p < 0.05$, ** $p < 0.01$ and *** $p < 0.001$. In vitro experiments were performed at least three times.

Figure 4. TMEM147 binds BCR and NF-κB p65.
(**A**) Control (Mock) and TMEM147-deficient ATDC5 (sh) cells were stimulated with or without TNF-α at the indicated time points. The phosphorylation of NF-κB p65 at S536 and IκBα was assessed by western blotting.
(**B**) Control (Mock) and TMEM147-deficient ATDC5 (sh) cells were stimulated with or without TNF-α at the indicated time points. The nuclear translocation of NF-κB p65 was examined by confocal microscopy. The cellular localization of NF-κB p65 as a percentage is shown (right). At least 200 cells were counted in each group. Scale bars: 20 μm.
(**C** and **D**) Control (Mock) and TMEM147-deficient ATDC5 (sh) cells were stimulated with or without TNF-α at the indicated time points. The phosphorylation of BCR at Y177 and CK2α at Y360 was assessed by western blotting.
(**E**) Control (Mock) and TMEM147-deficient ATDC5 (sh) cells were stimulated with or without TNF-α for 5 min, then immunoprecipitated with anti-NF-κB p65 to assess the phosphorylation of NF-κB p65 at S529.
(**F**) Flag-tagged TMEM147 was overexpressed in HEK293T cells. Following immunoprecipitation (IP) with anti-Flag beads, endogenous NF-κB p65, BCR and CK2α, as well as overexpressed TMEM147 were detected by immunoblotting (IB).
(**G**) Control (Mock) and TMEM147-deficient ATDC5 (sh) cells were stimulated with TNF-α for 5 min, then immunoprecipitated (IP) with anti-NF-κB p65. Finally, the samples were immunoblotted (IB) with anti-BCR or anti-NF-κB p65.
Experiments were performed at least three times; representative data are shown.

Figure 5. Anti-TMEM147 antibody suppresses the development of RA-like arthritis.
(**A**, **B** and **C**) ATDC5 cells were stimulated with human IL-6 plus sIL-6Rα and IL-17A in the presence or absence of anti-TMEM147 antibody. The mRNA levels of IL-6 (A) and CXCL1 (B), and protein levels of IL-6 (C) were measured. IL-6 production was measured by ELISA specific for mouse IL-6, which was not cross-reactive with human IL-6 added to the culture. Dot plots in (C) show cell growth measured by the MTT assay (right axis).
(**D**) The cytokine-induced arthritis model was prepared. Anti-TMEM147 antibody was injected into the ankle joints together with IL-6 and IL-17A. Clinical scores of the arthritis are shown (n = 5 per group).
(**E**) HE and Safranin-O staining of the ankle joints from the cytokine-induced arthritis model are shown. Scale bars: 100 μm.
(**F**) The percentage of Safranin-O (+) in the cartilage areas of (E).

(**G**) The mRNA level of IL-6 in the ankles of (D).
Data represent the mean ± S.D. (A-C, F and G) or S.E.M. (D). * $p < 0.05$, ** $p < 0.01$ and *** $p < 0.001$. In vitro and ex vivo experiments were performed at least three times.

Figure 6. Graphical abstract.
Activation of NF-κB p65 and STAT3 (the inflammation amplifier) in the chondrocytes of RA patients contributes to the collapse of articular homeostasis. TMEM147 acts as a scaffolding protein for binding NF-κB p65 with BCR, which facilitates the phosphorylation of NF-κB p65 at S529 and BCR at Y177 to activate the NF-κB signaling pathway. Target genes of the inflammation amplifier, such as cytokines, chemokines, growth factors, and the MMP and ADAMTS families contribute to the arthritis development.

Supplementary Figure 1. The inflammation amplifier synergistically enhances the expression of MMP13 and of ADAMTS5.

(**A** and **B**) Murine primary chondrocytes were stimulated with human IL-6 plus sIL-6Rα and/or TNF-α, and the mRNA levels of MMP13 (A) and ADAMTS5 (B) were measured.

Data represent the mean ± S.D. * $p < 0.05$ and ** $p < 0.01$. Experiments were performed at least three times.

Supplementary Figure 2. The inflammation amplifier exists in ATDC5.

(**A** and **B**) ATDC5 cells were stimulated with human IL-6 plus sIL-6Rα and/or IL-17A or TNF-α, and the mRNA (A) or protein (B) levels of IL-6 were measured to reveal activation of the inflammation amplifier. IL-6 production was measured by ELISA specific for mouse IL-6, which was not cross-reactive with human IL-6 added to the culture. Dot plots in (B) show cell growth measured by the MTT assay (right axis).

Data represent the mean ± S.D. *** $p < 0.001$. Experiments were performed at least three times.

Supplementary Figure 3. Computed tomography analysis for soft tissue swelling and bone destruction.

Each ankle specimen was scanned by computed tomography (CT).

(**A**) Wild type C57BL/6 mice (8-weeks old).

(**B-G**) The cytokine-induced arthritis model (cytokine-induced F759 arthritis) was prepared. Control antibody (B) or anti-TMEM147 antibody (C) was injected into the ankle joints together with IL-6 and IL-17A. F759 mice (D) or Col2Cre+ STAT3 flox/flox mice (E) were injected with IL-6 and IL-17A into the ankles. F759 that had received ankle injections of a lentivirus carrying non-target control shRNA sequence (F) or shRNA specific to TMEM147 (G) before IL-6 and IL-17A stimulation.

(**H** and **I**) The spontaneous RA model (12-month old F759 mice) was prepared. F759 mice (H) and Col2Cre+ STAT3 flox/flox mice (I) were inspected.

(**J** and **K**) The collagen-induced arthritis model in C57BL/6 mice (C57BL/6 CIA) was prepared. Control antibody (J) or anti-TMEM147 antibody (K) was injected into the ankle joints every three days starting 14 days after the first immunization.

Supplementary Figure 4. Inflammation amplifier activation and TMEM147 enhancement are observed in knee chondrocytes of F759 mice.

(**A**) Safranin-O staining and immunohistochemistry using anti-phospho-NF-κB p65 and phospho-STAT3 antibodies of the knee in the spontaneous RA model mice are shown (n = 5 per group). Scale bars: 100 μm.

(**B**) The percentage of Safranin-O (+) in the cartilage areas of (A).

(**C**) The percentage of cells showing phosphorylated NF-κB p65 and phosphorylated STAT3 in the cartilage areas. At least 200 cells were counted in each mouse.

(**D**) Immunohistochemistry using anti-TMEM147 antibody or control IgG of the knee joints (n = 5 per group). Scale bars: 100 μm.

Data represent the mean ± S.D. (B and C). *** $p < 0.001$.

Supplementary Figure 5. Inflammation amplifier activation in chondrocytes is important for RA development in mice.

(**A**) HE staining, Safranin-O staining and immunohistochemistry using anti-phospho-NF-κB p65 and phospho-STAT3 antibodies of the ankle in the cytokine-induced arthritis model are shown (n = 4-8 per group). Scale bars: 100 μm.

(**B**) The percentage of Safranin-O (+) in the cartilage areas of (A).

(**C**) The percentage of cells showing phosphorylated NF-κB p65 and phosphorylated STAT3 in the cartilage areas. At least 200 cells were counted in each mouse.
(**D**) Immunohistochemistry using anti-TMEM147 antibody or control IgG of the ankle joints (n = 5 per group). Scale bars: 100 μm.
Data represent the mean ± S.D. (B and C). * $p < 0.05$, ** $p < 0.01$ and *** $p < 0.001$.

Supplementary Figure 6. TMEM147 enhances NF-κB stimulation.
(**A** and **B**) Control (Mock) and TMEM147-overexpressing HEK293T cells were stimulated with or without TNF-α. The mRNA levels of TMEM147 (A) and of IL-6 (B) were measured.
Data represent the mean ± S.D. * $p < 0.05$ and *** $p < 0.001$. In vitro experiments were performed at least three times.

Supplementary Figure 7. Inflammation amplifier activation and cartilage degeneration are suppressed by TMEM147 knockdown in cytokine-induced arthritis in F759 mice.
The cytokine-induced arthritis model (cytokine-induced F759 arthritis) that received ankle injections of lentivirus carrying non-target control shRNA sequence (Mock) or shRNA specific to TMEM147 (sh TMEM147) before IL-6 and IL-17A stimulation.
(**A**) HE staining, Safranin-O staining and immunohistochemistry using anti-phospho-NF-κB p65, anti-phospho-STAT3 and anti-TMEM147 antibodies of the ankle (n = 4-8 per group). Scale bars: 100 μm.
(**B**) The percentage of Safranin-O (+) in the cartilage areas of (A) .
(**C**) The percentage of cells showing phosphorylated NF-κB p65 and phosphorylated STAT3 in the cartilage areas. At least 200 cells were counted in each mouse.
Data represent the mean ± S.D. (B and C). ** $p < 0.01$ and *** $p < 0.001$.

Supplementary Figure 8. Anti-TMEM147 antibody injection suppresses the inflammation amplifier activation in cytokine-induced arthritis in F759 mice.
(**A**) ATDC5 cells were treated with the generated anti-TMEM147 antibody, and TMEM147 expression on the cell surface was measured by flow cytometry.
(**B**) Immunohistochemistry using anti-phospho-NF-κB p65 and phospho-STAT3 antibodies of the ankle in the cytokine-induced arthritis model (cytokine-induced arthritis in F759) (n = 5 per group). Scale bars: 100 μm.
(**C**) The percentage of cells showing phosphorylated NF-κB p65 and phosphorylated STAT3 in the cartilage areas. At least 200 cells were counted in each mouse.
Data represent the mean ± S.D. (B and C). ** $p < 0.01$ and *** $p < 0.001$. In vitro experiments were performed at least three times.

Supplementary Figure 9. Anti-TMEM147 antibody suppresses the development of collagen-induced arthritis in C57BL/6 mice.
(**A**) The cytokine-induced arthritis model in C57BL/6 mice (C57BL/6 CIA) was prepared. Control antibody or anti-TMEM147 antibody was injected into the ankle joints every three days starting 14 days after the first immunization. Clinical scores of the arthritis are shown (n = 20 per group).
(**B**) HE staining and Safranin-O staining of the ankle joints. Scale bars: 100 μm.
(**C**) The percentage of Safranin-O (+) in the cartilage areas of (C).
Data represent the mean ± S.E.M. (A) or S.D. (C). * $p < 0.05$, ** $p < 0.01$ and *** $p < 0.001$.

Supplementary Figure 10. Inflammation amplifier activation and TMEM147 enhancement are observed in ankle chondrocytes of OA model.
(**A**) Safranin-O staining and immunohistochemistry using anti-phospho-NF-κB p65 and

phospho-STAT3 antibodies of the ankle in the spontaneous OA model mice (n = 5 per group). Scale bars: 100 μm.
(**B**) The percentage of Safranin-O (+) in the cartilage areas of (A).
(**C**) The percentage of cells showing phosphorylated NF-κB p65 and phosphorylated STAT3 in the cartilage areas. At least 200 cells were counted in each mouse.
(**D**) Immunohistochemistry using anti-TMEM147 antibody or control IgG of the ankle joints (n = 5 per group). Scale bars: 100 μm.
Data represent the mean ± S.D. (B and C). *** $p < 0.001$.

Supplementary Figure 11. Inflammation amplifier activation and TMEM147 enhancement are observed in knee chondrocytes of an OA model.
(**A**) Safranin-O staining and immunohistochemistry using anti-phospho-NF-κB p65 and phospho-STAT3 antibodies of the knee in spontaneous OA model mice are shown (n = 5 per group). Scale bars: 100 μm.
(**B**) The percentage of Safranin-O (+) in the cartilage areas of (A).
(**C**) The percentages of cell showing phosphorylated NF-κB p65 and phosphorylated STAT3 in cartilage areas. At least 200 cells were counted in each mouse.
(**D**) Immunohistochemistry using anti-TMEM147 antibody or control IgG of knee joints from spontaneous OA models (n = 5 per group). Scale bars: 100 μm.
Data represent the mean ± S.D. (B and C). * $p < 0.05$, ** $p < 0.01$ and *** $p < 0.001$.

Supplementary Figure 12. Enhanced activation of the inflammation amplifier and TMEM147 enhancement are observed in chondrocytes from OA patients.
(**A**) Safranin-O staining and immunohistochemistry using anti-phospho-NF-κB p65 and phospho-STAT3 antibodies of knee joints in patients with polydactyly (control) or OA are shown (n = 5 per group). Scale bars: 100 μm.
(**B**) The percentage of cells showing phosphorylated NF-κB p65 and phosphorylated STAT3 in cartilage areas. At least 200 cells were counted in each patient.
(**C**) Immunohistochemistry using anti-TMEM147 antibody or control IgG of knee joints in patients with polydactyly (control) or OA (n = 5 per group). Scale bars: 100 μm.
Data represent the mean ± S.D. *** $p < 0.001$.

Supplementary Table 1. Information of patients.
Rt, right; Lt, left.

Supplementary Table 2. Primer sequences used in this study.

References

1. Makris EA, Gomoll AH, Malizos KN, et al. Repair and tissue engineering techniques for articular cartilage. *Nat Rev Rheumatol* 2015;11(1):21-34. doi: 10.1038/nrrheum.2014.157
2. Smolen JS, Aletaha D. Rheumatoid arthritis therapy reappraisal: strategies, opportunities and challenges. *Nat Rev Rheumatol* 2015;11(5):276-89. doi: 10.1038/nrrheum.2015.8 [published Online First: 2015/02/17]
3. Pap T, Korb-Pap A. Cartilage damage in osteoarthritis and rheumatoid arthritis--two unequal siblings. *Nat Rev Rheumatol* 2015;11(10):606-15. doi: 10.1038/nrrheum.2015.95
4. Smolen JS, Aletaha D, Redlich K. The pathogenesis of rheumatoid arthritis: new insights from old clinical data? *Nat Rev Rheumatol* 2012;8(4):235-43. doi: 10.1038/nrrheum.2012.23 [published Online First: 2012/03/13]
5. Bartok B, Firestein GS. Fibroblast-like synoviocytes: key effector cells in rheumatoid arthritis. *Immunol Rev* 2010;233(1):233-55. doi: 10.1111/j.0105-2896.2009.00859.x
6. Hotamisligil GS. Inflammation and metabolic disorders. *Nature* 2006;444:860-67.
7. Glass CK, Saijo K, Winner B, et al. Mechanisms underlying inflammation in neurodegeneration. *Cell* 2010;140(6):918-34. doi: 10.1016/j.cell.2010.02.016
8. Murakami M, Harada M, Kamimura D, et al. Disease-association analysis of an inflammation-related feedback loop. *Cell Rep* 2013;3(3):946-59. doi: 10.1016/j.celrep.2013.01.028
9. Atsumi T, Singh R, Sabharwal L, et al. Inflammation amplifier, a new paradigm in cancer biology. *Cancer Research* 2014;74:8-14. doi: 10.1158/0008-5472.CAN-13-2322
10. Murakami M, Kamimura D, Hirano T. Pleiotropy and Specificity: Insights from the Interleukin 6 Family of Cytokines. *Immunity* 2019;50(4):812-31. doi: 10.1016/j.immuni.2019.03.027
11. Lee J, Nakagiri T, Kamimura D, et al. IL-6 amplifier activation in epithelial regions of bronchi after allogeneic lung transplantation. *Int Immunol* 2013;25(5):319-32. doi: 10.1093/intimm/dxs158
12. Fujita M, Yamamoto Y, Jiang JJ, et al. NEDD4 Is Involved in Inflammation Development during Keloid Formation. *J Invest Dermatol* 2019;139(2):333-41. doi: 10.1016/j.jid.2018.07.044 [published Online First: 2018/10/03]
13. Weisberg E, Manley PW, Cowan-Jacob SW, et al. Second generation inhibitors of BCR-ABL for the treatment of imatinib-resistant chronic myeloid leukaemia. *Nat Rev Cancer* 2007;7(5):345-56. doi: 10.1038/nrc2126
14. Meng J, Jiang JJ, Atsumi T, et al. Breakpoint Cluster Region-Mediated Inflammation Is Dependent on Casein Kinase II. *J Immunol* 2016;197(8):3111-19. doi: 10.4049/jimmunol.1601082
15. Dettmer U, Kuhn PH, Abou-Ajram C, et al. Transmembrane protein 147 (TMEM147) is a novel component of the Nicalin-NOMO protein complex. *J Biol Chem* 2010;285(34):26174-81. doi: 10.1074/jbc.M110.132548
16. Atsumi T, Ishihara K, Kamimura D, et al. A point mutation of Tyr-759 in interleukin 6 family cytokine receptor subunit gp130 causes autoimmune arthritis. *J Exp Med* 2002;196(7):979-90. [published Online First: 2002/10/09]
17. Takeda K, Kaisho T, Yoshida N, et al. Stat3 activation is responsible for IL-6-dependent T cell proliferation through preventing apoptosis: generation and characterization of T cell-specific Stat3-deficient mice. *J Immunol* 1998;161(9):4652-60. [published Online First: 1998/10/30]
18. Sawa S, Kamimura D, Jin GH, et al. Autoimmune arthritis associated with mutated interleukin (IL)-6 receptor gp130 is driven by STAT3/IL-7-dependent homeostatic proliferation of CD4+ T cells. *J Exp Med* 2006;12:1459-70.
19. Murakami M, Okuyama Y, Ogura H, et al. Local microbleeding facilitates IL-6- and

734 IL-17-dependent arthritis in the absence of tissue antigen recognition by activated T cells. *J*
735 *Exp Med* 2011;208(1):103-14. doi: jem.20100900 [pii]
736 10.1084/jem.20100900 [published Online First: 2011/01/12]
737 20. Harada M, Kamimura D, Arima Y, et al. Temporal expression of growth factors triggered by
738 epiregulin regulates inflammation development. *J Immunol* 2015;194(3):1039-46. doi:
739 10.4049/jimmunol.1400562
740 21. Atsumi T, Suzuki H, Jiang JJ, et al. Rbm10 regulates inflammation development via alternative
741 splicing of Dnmt3b. *Int Immunol* 2017;29(12):581-91. doi: 10.1093/intimm/dxx067
742 22. Okuyama Y, Tanaka Y, Jiang JJ, et al. Bmi1 Regulates IkappaBalpha Degradation via Association
743 with the SCF Complex. *J Immunol* 2018;201(8):2264-72. doi: 10.4049/jimmunol.1701223
744 [published Online First: 2018/09/14]
745 23. Tanaka Y, Sabharwal L, Ota M, et al. Presenilin 1 Regulates NF-kappaB Activation via
746 Association with Breakpoint Cluster Region and Casein Kinase II. *J Immunol*
747 2018;201(8):2256-63. doi: 10.4049/jimmunol.1701446 [published Online First: 2018/09/12]
748 24. Stoop R, van der Kraan PM, Buma P, et al. Type II collagen degradation in spontaneous
749 osteoarthritis in C57Bl/6 and BALB/c mice. *Arthritis Rheum* 1999;42(11):2381-9. doi:
750 10.1002/1529-0131(199911)42:11<2381::AID-ANR17>3.0.CO;2-E
751 25. Gosset M, Berenbaum F, Thirion S, et al. Primary culture and phenotyping of murine
752 chondrocytes. *Nat Protoc* 2008;3(8):1253-60. doi: 10.1038/nprot.2008.95
753 26. Ehlers M, Grotzinger J, deHon FD, et al. Identification of two novel regions of human IL-6
754 responsible for receptor binding and signal transduction. *J Immunol* 1994;153(4):1744-53.
755 27. Ogura H, Murakami M, Okuyama Y, et al. Interleukin-17 Promotes Autoimmunity by Triggering
756 a Positive-Feedback Loop via Interleukin-6 Induction. *Immunity* 2008;29:628-36. doi:
757 10.1016/j.immuni.2008.07.018
758 28. Lee J, Nakagiri T, Oto T, et al. IL-6 amplifier, NF-kappaB-triggered positive feedback for IL-6
759 signaling, in grafts is involved in allogeneic rejection responses. *J Immunol*
760 2012;189(4):1928-36. doi: jimmunol.1103613 [pii]
761 10.4049/jimmunol.1103613 [published Online First: 2012/07/17]
762 29. Narimatsu M, Maeda H, Itoh S, et al. Tissue-specific autoregulation of the stat3 gene and its role
763 in interleukin-6-induced survival signals in T cells. *Mol Cell Biol* 2001;21(19):6615-25.
764 [published Online First: 2001/09/05]
765 30. Ghoreschi K, Laurence A, Yang XP, et al. Generation of pathogenic T(H)17 cells in the absence
766 of TGF-beta signalling. *Nature* 2010;467(7318):967-71. doi: nature09447 [pii]
767 10.1038/nature09447 [published Online First: 2010/10/22]
768 31. Krzeski P, Buckland-Wright C, Balint G, et al. Development of musculoskeletal toxicity without
769 clear benefit after administration of PG-116800, a matrix metalloproteinase inhibitor, to
770 patients with knee osteoarthritis: a randomized, 12-month, double-blind, placebo-controlled
771 study. *Arthritis Res Ther* 2007;9(5):R109. doi: 10.1186/ar2315
772 32. Rosemond E, Rossi M, McMillin SM, et al. Regulation of M(3) muscarinic receptor expression
773 and function by transmembrane protein 147. *Mol Pharmacol* 2011;79(2):251-61. doi:
774 10.1124/mol.110.067363
775

Figure 1

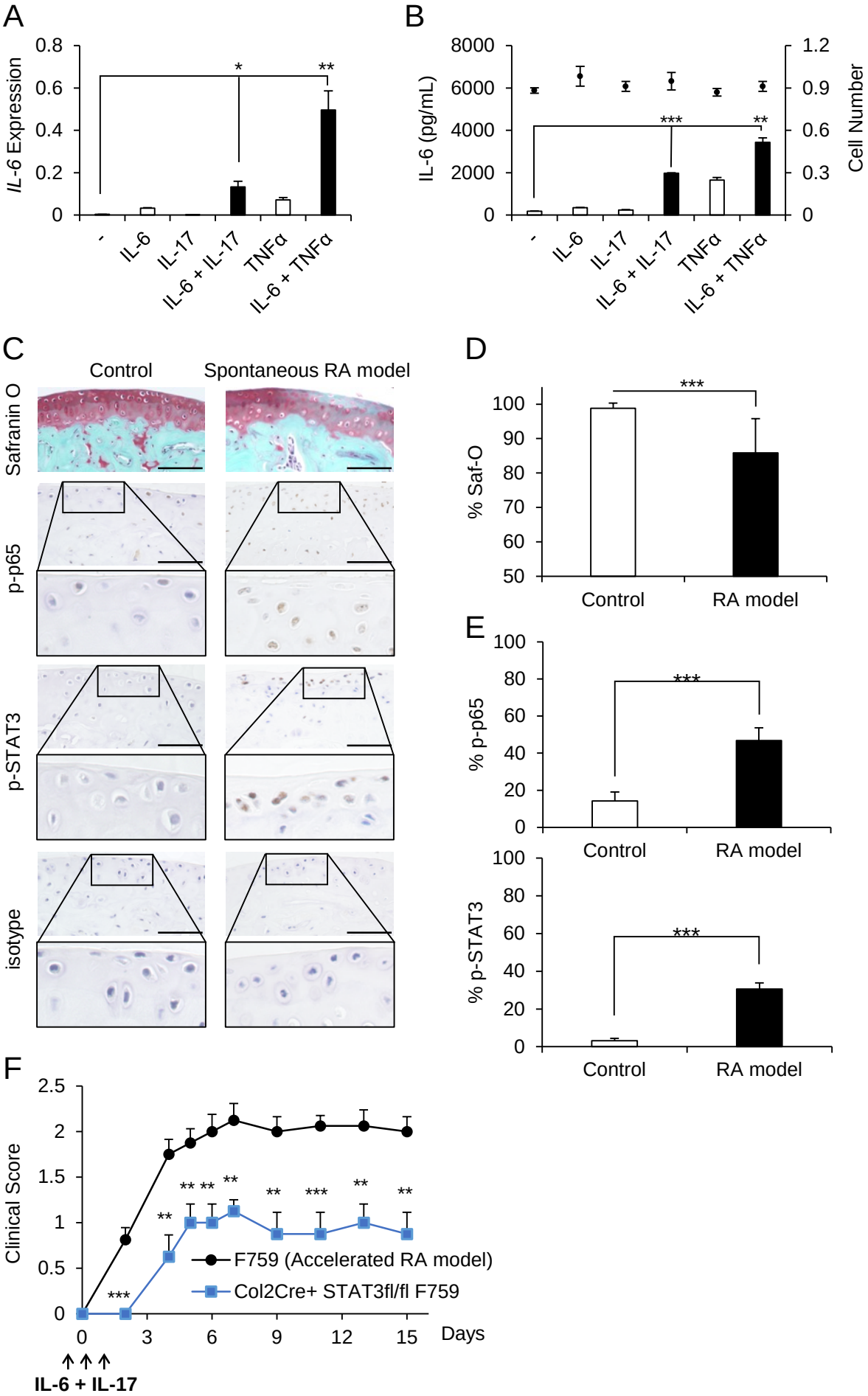
A
IL-6 Expression
0.8
0.6
0.4
0.2
0
*
**
-
IL-6
IL-17
IL-6 + IL-17
TNFα
IL-6 + TNFα
B
IL-6 (pg/mL)
8000
6000
4000
2000
0
Cell Number
1.2
0.9
0.6
0.3
0
***
**
C
Control
Spontaneous RA model
Safranin O
p-p65
p-STAT3
isotype
D
% Saf-O
100
90
80
70
60
50
***
Control
RA model
E
% p-p65
100
80
60
40
20
0
***
Control
RA model
% p-STAT3
100
80
60
40
20
0
***
Control
RA model
F
Clinical Score
2.5
2
1.5
1
0.5
0
0
3
6
9
12
15
Days
F759 (Accelerated RA model)
Col2Cre+ STAT3fl/fl F759
IL-6 + IL-17

A

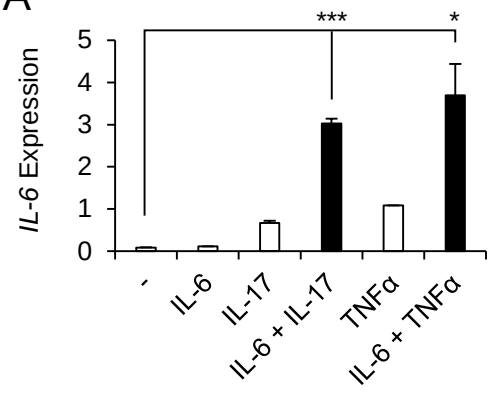
***
*
IL-6 Expression
5
4
3
2
1
0
-
IL-6
IL-17
IL-6 + IL-17
TNFα
IL-6 + TNFα

B

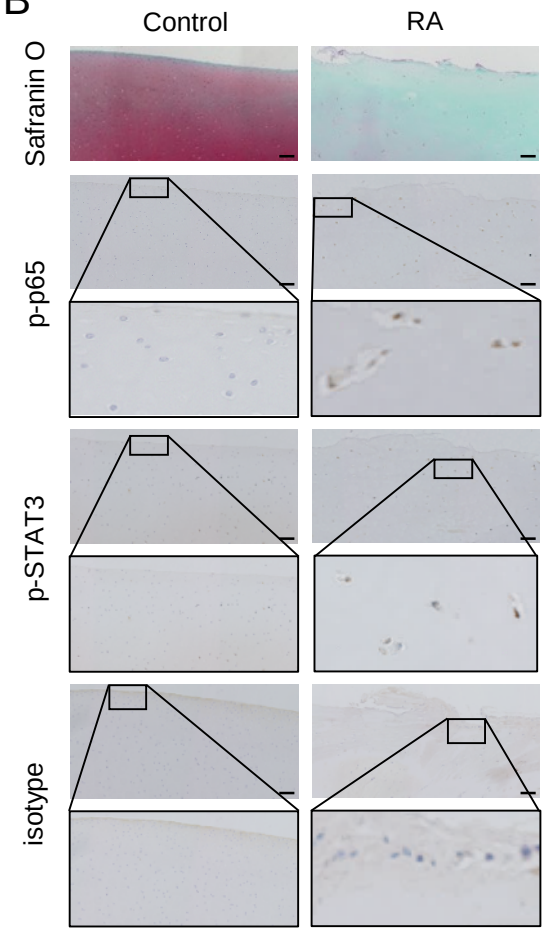
Control
RA
Safranin O
p-p65
p-STAT3
isotype

C

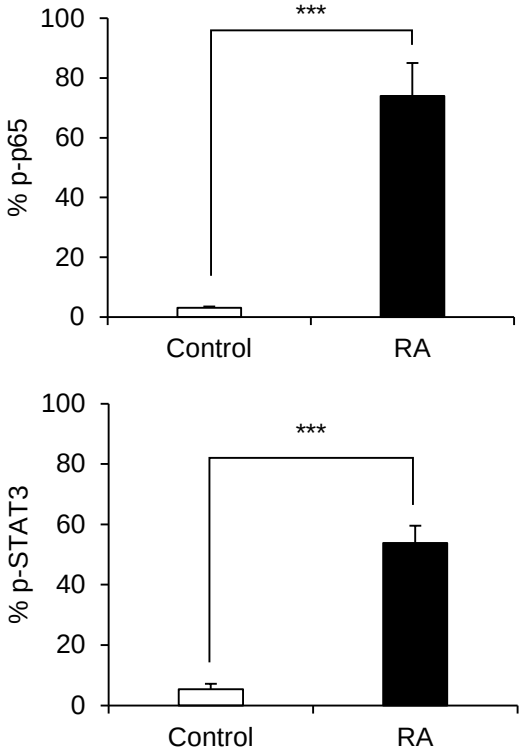
***
% p-p65
100
80
60
40
20
0
Control
RA
***
% p-STAT3
100
80
60
40
20
0
Control
RA

Figure 3

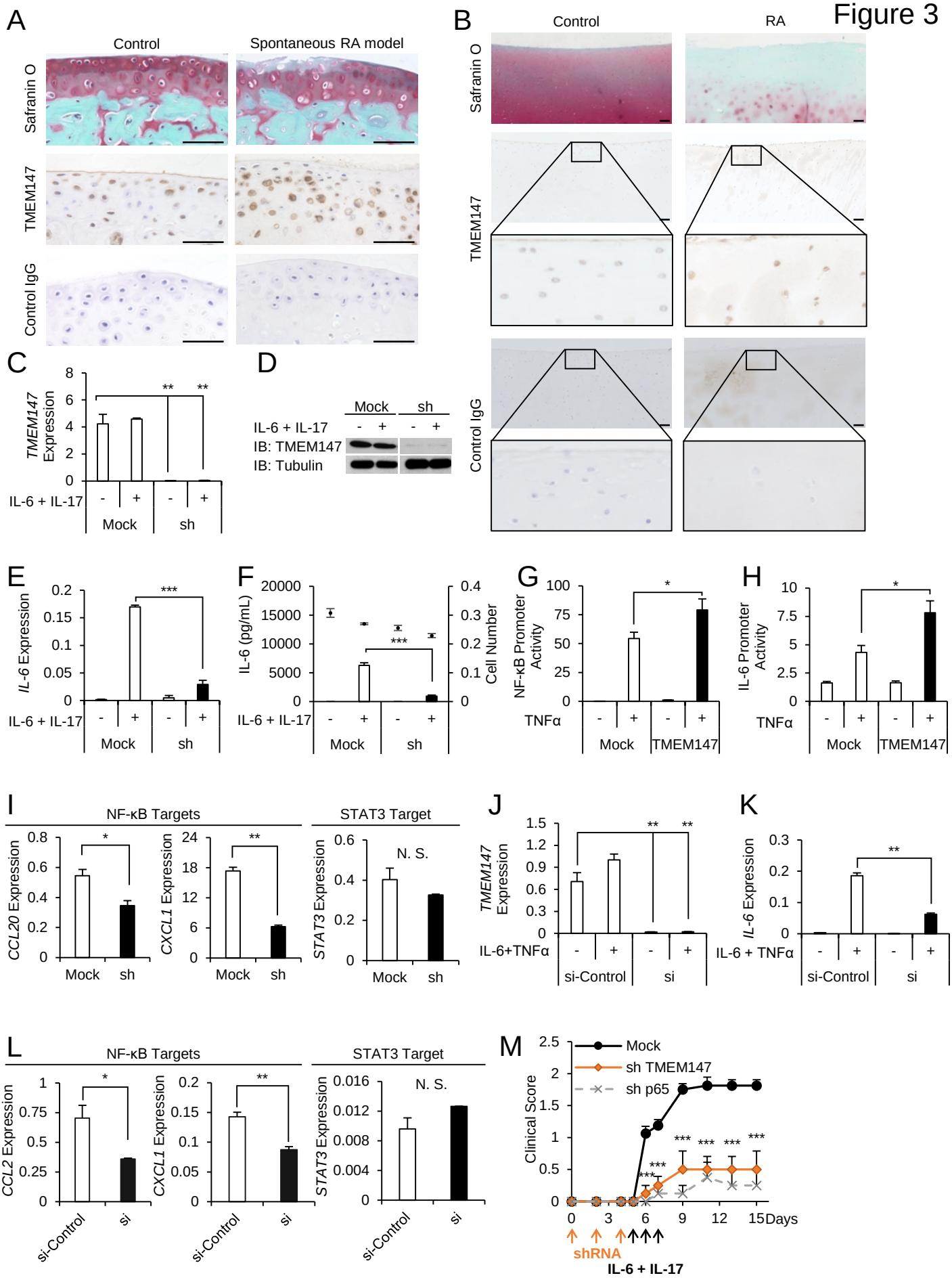
A
Control
Spontaneous RA model
Safranin O
TMEM147
Control IgG
B
Control
RA
Safranin O
TMEM147
Control IgG
C
TMEM147 Expression
IL-6 + IL-17
Mock
sh
D
Mock
sh
IL-6 + IL-17
IB: TMEM147
IB: Tubulin
E
IL-6 Expression
IL-6 + IL-17
Mock
sh
F
IL-6 (pg/mL)
Cell Number
IL-6 + IL-17
Mock
sh
G
NF-κB Promoter Activity
TNFα
Mock
TMEM147
H
IL-6 Promoter Activity
TNFα
Mock
TMEM147
I
NF-κB Targets
STAT3 Target
CCL20 Expression
CXCL1 Expression
STAT3 Expression
N. S.
Mock
sh
J
TMEM147 Expression
IL-6+TNFα
si-Control
si
K
IL-6 Expression
IL-6 + TNFα
si-Control
si
L
NF-κB Targets
STAT3 Target
CCL2 Expression
CXCL1 Expression
STAT3 Expression
N. S.
si-Control
si
M
Mock
sh TMEM147
sh p65
Clinical Score
Days
shRNA
IL-6 + IL-17

Figure 4

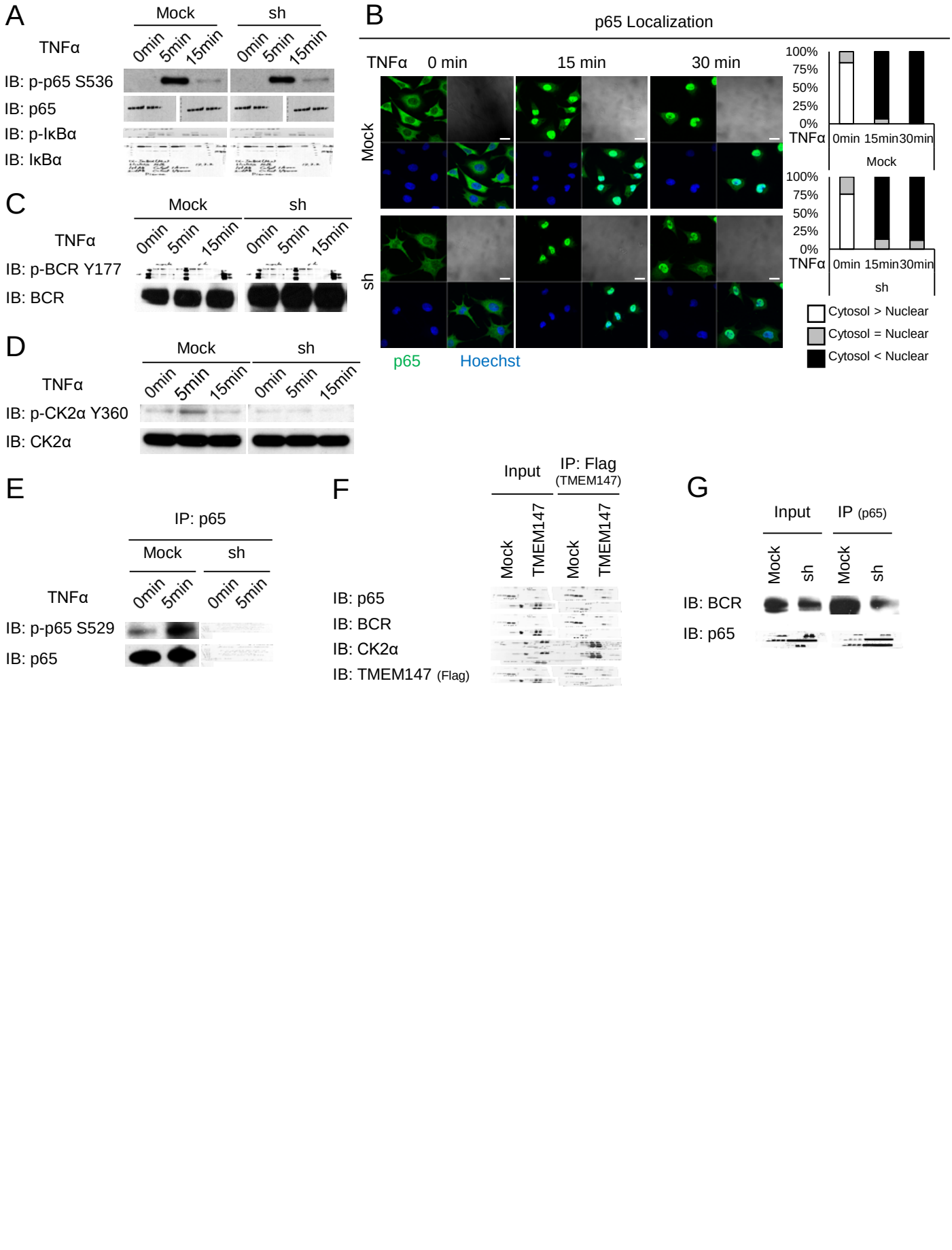
A
Mock
sh
TNFα
0min
5min
15min
IB: p-p65 S536
IB: p65
IB: p-IκBα
IB: IκBα
B
p65 Localization
TNFα
0 min
15 min
30 min
Mock
sh
p65
Hoechst
100%
75%
50%
25%
0%
0min
15min
30min
Cytosol > Nuclear
Cytosol = Nuclear
Cytosol < Nuclear
C
IB: p-BCR Y177
IB: BCR
D
IB: p-CK2α Y360
IB: CK2α
E
IP: p65
IB: p-p65 S529
IB: p65
F
Input
IP: Flag
(TMEM147)
IB: p65
IB: BCR
IB: CK2α
IB: TMEM147 (Flag)
G
IP (p65)
IB: BCR
IB: p65

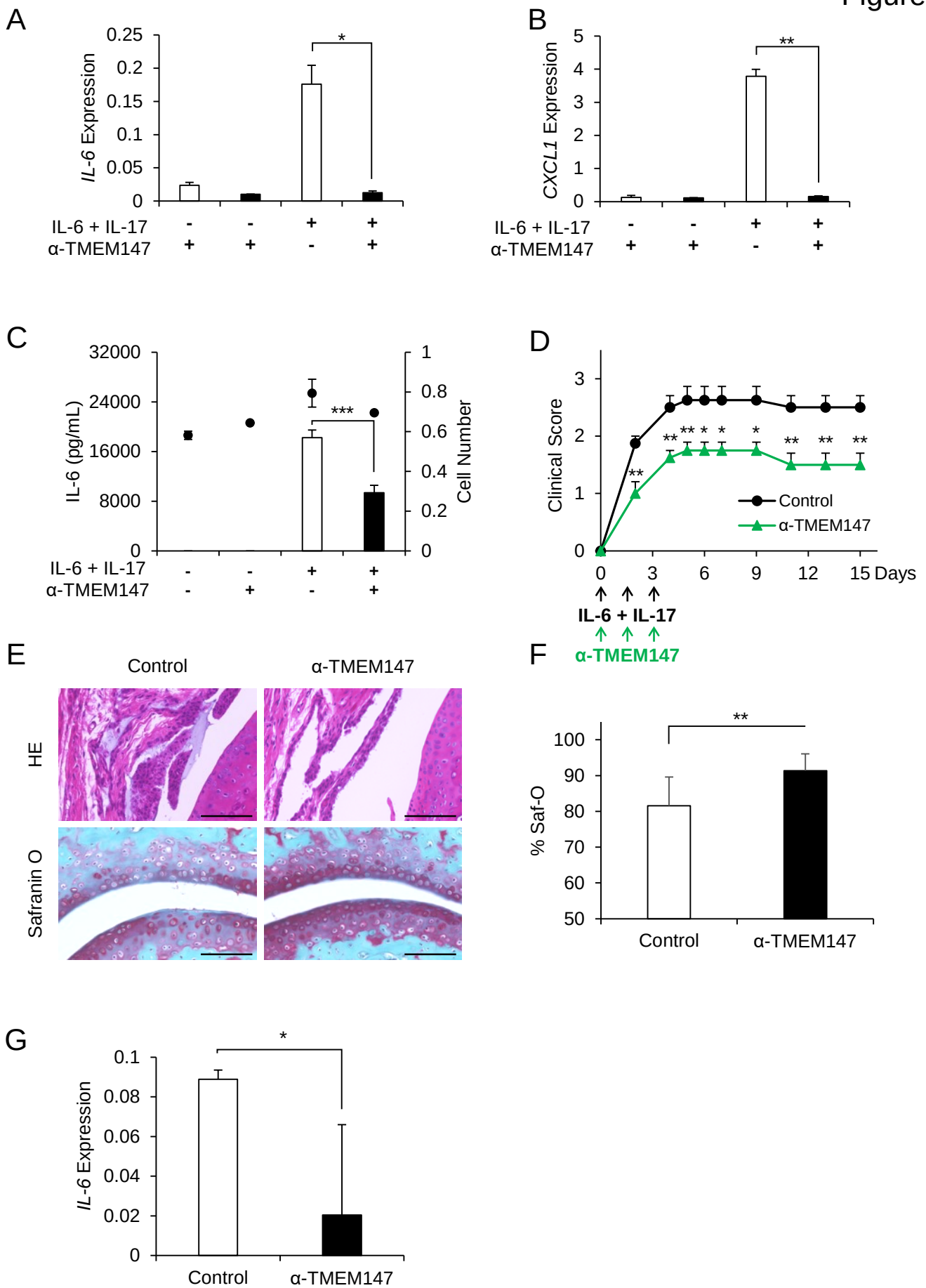
A
IL-6 Expression
0.25
0.2
0.15
0.1
0.05
0
*
IL-6 + IL-17 - - + +
α-TMEM147 + + - +
B
CXCL1 Expression
5
4
3
2
1
0
**
IL-6 + IL-17 - - + +
α-TMEM147 + + - +
C
IL-6 (pg/mL)
32000
24000
16000
8000
0
Cell Number
1
0.8
0.6
0.4
0.2
0
***
IL-6 + IL-17 - - + +
α-TMEM147 - + - +
D
Clinical Score
3
2
1
0
Control
α-TMEM147
0 3 6 9 12 15 Days
IL-6 + IL-17
α-TMEM147
E
Control
α-TMEM147
HE
Safranin O
F
% Saf-O
100
90
80
70
60
50
**
Control
α-TMEM147
G
IL-6 Expression
0.1
0.08
0.06
0.04
0.02
0
*
Control
α-TMEM147

Rheumatoid Arthritis